International Journal of Computer Trends and Technology
ISSN: 2231–2803 / https://doi.org/10.14445/22312803/IJCTT-V73I11P107

Volume 73 Issue 11, 43-54, November 2025

Original Article

Impact of Foreign-Continuum Scaling on Terahertz (THz) Link Performance: Bridging High-Resolution Modeling and System-Level Metrics

Ahmed Sidi Aman[1], Ramafiarisona Hajasoa Malala[2]

[1,2]*STII TASI, University of Antananarivo, Madagascar.*

Corresponding Author : engineer.sidi@gmail.com

Received: 21 September 2025 Revised: 29 October 2025 Accepted: 16 November 2025 Published: 30 November 2025

Abstract - *This work extends a previously developed high-resolution Line-By-Line (LBL) framework to quantify how a calibrated Foreign-Continuum Scaling S(f) affects outdoor THz link performance. The spectroscopic structure is unchanged—HITRAN line absorption, MT_CKD self/foreign continua, and dry collision-induced absorption—while S(f) is applied* ***only*** *to the foreign continuum. The correction follows an affine frequency trend, is windowed over 600–980 GHz, and activates only where the foreign continuum dominates, avoiding line-dominated regions. The focus is placed on the practical implications of S(f) for link behavior under varying atmospheric conditions. Using three representative humidity–temperature scenarios (dry, moderate, humid) and link distances up to 1 km, the analysis examines how minor spectral deviations translate into key communication metrics such as Received Signal Level (RSL), Signal-to-Noise Ratio (SNR), and capacity. Below 600 GHz, LBL and LBL×S(f) produce nearly identical results. Above that, especially in bands Z4–Z5, differences grow more significant as continuum effects begin to dominate. Linking spectroscopic accuracy to link-budget modeling shows that the foreign continuum must be explicitly accounted for in both spectroscopic analyses and system-level design.*

Keywords - *Terahertz Links, Line-by-Line Modeling, Water-Vapor Continuum, Foreign Continuum Scaling, Atmospheric Attenuation, Link Budget Analysis.*

1. Introduction

Short-range, high-throughput wireless links in the 0.3–1 THz band are increasingly considered for future systems. [1] Use cases such as backhaul, fronthaul, and ultra-broadband access in post-5G and 6G networks could benefit from the broad, continuous bandwidth available across this range. [2]

However, practical use is challenging because atmospheric attenuation varies strongly with frequency and limits the range. This frequency-dependent loss is not incidental. Even minor modeling mismatches can end up shifting key performance estimates like Received Signal Level (RSL), Signal-to-Noise Ratio (SNR), and link capacity.

A previous study introduced a physics-based, high-resolution LBL model that decomposes absorption into line, continuum (self/foreign), and dry-air CIA terms. [3] When this model was compared with established references such as the Atmospheric Model (AM) and ITU-R P.676, a consistent underestimation of the foreign-broadened continuum was observed in the upper-sub-THz region. To address that, and without affecting the behavior of well-resolved spectral lines, a frequency-dependent Scaling Function S(f) was explicitly applied to the foreign continuum.

The correction is confined to foreign-continuum-dominated regions, follows an affine trend over 600–980 GHz, and is amplitude-limited. This adjustment improved agreement between modeled α(f) and experimental data, as well as with AM and ITU-R reference spectra.

Since spectroscopic models are still being developed, limited research has been done to quantify the precise way in which these continuum-level disparities translate into system-level measures. Rather than the operational influence on wireless channels, most of the current research concentrates on spectral matching. As a result, it is still unclear how much continuum uncertainty influences outdoor link dimensioning, particularly regarding range and availability.

This study builds directly on that foundation, but shifts the focus to the system level. The objective is to quantify how the correction affects link behavior across the Z_1–Z_5 windows. The analysis considers three representative atmospheric

conditions: dry, moderate, and humid, corresponding to water vapor densities of roughly 3.6, 8.0, and 15.0 g/m³. Link distances of 100, 500, and 1000 meters are tested under consistent system parameters: EIRP = 55 dBm, G_rx = 50 dBi, B = 1 GHz, NF = 6 dB, and T_sys = 290 K.

Three main effects are studied:

- Frequency selectivity: Z_1–Z_3 (300–525 GHz) are still driven mainly by molecular absorption and remain usable, while Z_4–Z_5 become more sensitive to continuum uncertainty. [4]
- Range accumulation: small modeling errors increase with distance and degrade performance over longer links.
- Continuum calibration: accurate tuning of foreign-continuum parameters becomes key when building THz link budgets or defining standards. [5]

The remaining parts of the paper provide a modeling approach, simulation configuration, and link-level results observed between different humidity levels, including Z_4 and Z_5. The last two sections represent practical recommendations for outdoor THz deployment, focusing on achievable frequency bands, distance targets to be reached, and suggestions for including continuum effects in system design.

2. Methodology and study parameters

The entire modeling pipeline that links comprehensive spectroscopic absorption data to telecom-level link-budget metrics is processed on a single frequency grid and described in this section. Physical absorption components are isolated using a Line-By-Line (LBL) decomposition on the first step of the operation. Discrete spectral lines are preserved by selectively applying a frequency-dependent Scaling Factor S(f) to the foreign water vapor continuum. Local disparities are contextualized by calculating AM v14 and ITU-R P.676 on the same grid as external baselines for comparison and validation. [9] Under consistent radio assumptions, atmospheric attenuation and free-space path loss are then converted into three important link metrics: Received Signal Level (RSL), Signal-to-Noise Ratio (SNR), and the Shannon Capacity C(f). This setup isolates continuum calibration effects from the discrete line structure. All quantities are evaluated on a standard grid $f \in [300{,}1000]$ GHz with $\Delta f = 0.05$ GHz. The analysis focuses on five canonical windows: Z1 (300–375 GHz), Z2 (385–440 GHz), Z3 (460–525 GHz), Z4 (620–710 GHz), and Z5 (820–900 GHz). Whereas Z1–Z3 remain densely line-populated, Z4 and Z5 are characterized by wider line spacing and a stronger role of the absorption baseline; consequently, any bias in the foreign continuum is expected to have greater influence there on link-level behavior.

Atmospheric variability is represented by three clear-air humidity cases at $T = 296$ K and ≈ 1 atm, specified by H_2O Volume-Mixing Ratio (VMR) and approximate water-vapor density ρ_w: Case 1 (dry) with $\mathrm{VMR}(H_2O) = 0.00485$ and $\rho_w \approx 3.60\ \mathrm{g\,m^{-3}}$; Case 2 (moderate) with 0.01080 and $8.01\ \mathrm{g\,m^{-3}}$; and Case 3 (humid) with 0.02020 and $14.98\ \mathrm{g\,m^{-3}}$. Three line-of-sight distances are considered, $L \in \{100{,}500{,}1000\}$ m, representative of short-range backhaul and access. The propagation scenario assumes clear-air, line-of-sight conditions without hydrometeors or aerosols (no rain, fog, cloud, or particulate scattering) and excludes pointing errors, phase noise, and RF non-linearities.

The continuum scaling follows the calibration logic established in the previous work and is both selective and line-neutral. Let $S_{\mathrm{lin}}(f) = A + B\, f_{\mathrm{GHz}}$ with $A = 3.7830$ and $B = -0.001206$. A raised-cosine apodization $W(f)$ confines the support to 600–980 GHz (ramp 600–720, plateau 720–930, ramp-down 930–980). The effective factor

$$S_{\mathrm{eff}}(f) = 1 + \gamma\, W(f)\,(S_{\mathrm{lin}}(f) - 1), \qquad \gamma = 0.60,$$

is applied only where the foreign-continuum fraction

$$\frac{\alpha_{\mathrm{foreign}}(f)}{\alpha_{\mathrm{foreign}}(f) + \alpha_{\mathrm{self}}(f)} \geq 0.60$$

indicates dominance; outside this condition (or outside the apodized band), $S_{\mathrm{eff}}(f) = 1$. A safety clamp enforces $S_{\mathrm{eff}}(f) \in [0.70,\ 3.50]$. The total absorption with correction is then

$$\alpha_{\mathrm{LBL}\times S}(f) = \alpha_{\mathrm{lines}}(f) + \alpha_{\mathrm{self}}(f) + S_{\mathrm{eff}}(f)\,\alpha_{\mathrm{foreign}}(f) + \alpha_{\mathrm{dry}}(f),$$

Which preserves the positions and depths of line notches while adjusting the inter-line floor only where the foreign continuum is physically expected to dominate. AM v14 and ITU-R P.676 curves serve purely as external spectral references. AM v14 and ITU-R P.676 are computed and used solely as external spectral references (AM preferred; ITU used if AM is unavailable). Link-level quantities are continuously computed from the LBL family (bare LBL and LBL$\times S(f)$) so that the impact of continuum calibration is isolated rather than blended with external models.

Radio parameters are held fixed to avoid conflating equipment choices with propagation: EIRP $= 55$ dBm, $G_{\mathrm{rx}} = 50$ dBi, $B = 1$ GHz, NF $= 6$ dB, and $T_{\mathrm{sys}} = 290$ K. Let $\alpha(f)$ denote the power-attenuation coefficient in $\mathrm{m^{-1}}$. Over a path L, atmospheric loss is

$$A_{\mathrm{atm}}(f, L) = \frac{10}{\ln 10}\,\alpha(f)\,L \approx 4.342945\,\alpha(f)\,L \quad \text{(dB)},$$

and free-space loss is

$$\mathrm{FSPL}(f,L) = 20\log_{10}(4\pi fL/c) \quad \text{(dB)}, \qquad f \text{ in Hz. [10]}$$

The received level follows as

$$\mathrm{RSL}(f) = \mathrm{EIRP} + G_{\mathrm{rx}} - \mathrm{FSPL}(f,L) - A_{\mathrm{atm}}(f,L) \quad \text{(dBm)},$$

with thermal-noise power over bandwidth B

$$N_{\mathrm{dBm}} = -174 + 10\log_{10}B + \mathrm{NF} + 10\log_{10}\left(T_{\mathrm{sys}}/290\right) \quad \text{(dBm)}.$$

Hence,

$$\mathrm{SNR}(f) = \mathrm{RSL}(f) - N_{\mathrm{dBm}} \quad \text{(dB)},$$

$$C(f) = \frac{B}{10^9}\log_2\left(1 + 10^{\mathrm{SNR}(f)/10}\right) \quad \text{(Gb/s). [11]}$$

For interpretation, a conservative demodulation threshold such as SNR_min = 6 dB can be added for reference, though the continuous capacity curve is preserved to reflect how absorption gradually affects throughput.

2.1. Spectral Baselines and Guarded Continuum Correction LBL Decomposition

The absorption coefficient $\alpha(f)$ is evaluated on a standard grid $f \in [300,1000]$ GHz with step $\Delta f = 0.05$ GHz. The formulation remains strictly decomposable: each physical contribution is independently computed at the case thermodynamic state ($T = 296$ K, $p \approx 1$ atm) and then combined additively in the power-attenuation domain (m^{-1}). Line absorption for H2O and O2 is obtained from HITRAN using exact Voigt evaluation, yielding $\alpha\mathrm{lines}(f)$. [6] The water-vapor continuum is based on MT_CKD 4.3, with self and foreign components generated under the same conditions, interpolated onto the grid, and expressed in m^{-1}, resulting in $\alpha\mathrm{self}(f)$ and $\alpha_{\mathrm{foreign}}(f)$; the total continuum is $\alpha_{(\mathrm{H2O,cont})}(f) = \alpha\mathrm{self}(f) + \alpha_{\mathrm{foreign}}(f)$. [7] The dry-air collision-induced background (Debye-like O2 and N2 CIA) follows ITU-R P.676 and is denoted $\alpha\mathrm{dry}(f)$. [8] The complete line-by-line assembly is thus $\alpha\mathrm{LBL}(f) = \alpha_{\mathrm{lines}}(f) + \alpha_{(\mathrm{H2O,cont})}(f) + \alpha\mathrm{dry}(f)$, with all quantities in m^{-1} for direct path-loss conversion.

A guarded, foreign-only Scaling $S(f)$ is introduced to explore a potential high-frequency shortfall in the continuum. The corrected coefficient is

$\alpha_{(\mathrm{LBL}\times S)}(f) = \alpha_{\mathrm{lines}}(f) + \alpha_{\mathrm{self}}(f) + S_{\mathrm{eff}}(f), \alpha_{\mathrm{foreign}}(f) + \alpha_{\mathrm{dry}}(f)$,

Where $S_{\mathrm{lin}}(f) = A + B, f_{\mathrm{GHz}}$ (with $A = 3.7830$, $B = -0.001206$) defines an affine trend, a raised-cosine Window $W(f)$ confines support to 600–980 GHz (ramp 600–720, plateau 720–930, ramp-down 930–980), and a damping factor $\gamma = 0.60$ gives $S_{\mathrm{eff}}(f) = 1 + \gamma, W(f), [S_{\mathrm{lin}}(f) - 1]$. Activation is restricted to frequencies where the foreign-continuum fraction dominates, $\frac{\alpha_{\mathrm{foreign}}(f)}{\alpha_{\mathrm{self}}(f)+\alpha_{\mathrm{foreign}}(f)} \geq 0.60$, otherwise $S_{\mathrm{eff}}(f) = 1$; a safety clamp enforces $S_{\mathrm{eff}}(f) \in [0.70,,3.50]$. By construction, the correction is line-neutral and does not affect the self continuum or the dry CIA term; it leaves Z1–Z3 essentially untouched and focuses the probe on sub-bands where the foreign continuum is physically influential (primarily Z5 and parts of Z4).

For spectral context, AM v14 and ITU-R P.676 absorptions are computed and used strictly as external references (AM prioritized, ITU fallback if needed). [6] Link-budget quantities are derived from the LBL pair $\alpha_{\mathrm{LBL}},, \alpha_{(\mathrm{LBL}\times S)}$ to isolate sensitivity to continuum calibration without blending modelling frameworks. All $\alpha(\cdot)$ terms are in m^{-1}; when expressed in dB, path attenuation is given by $A_{\mathrm{atm}}(f,L) = \frac{10}{\ln 10}, \alpha(f), L \approx 4.342945, \alpha(f), L$ with L in meters; frequency is expressed in GHz unless otherwise noted.

2.2. Telecom Mapping and Evaluation Protocol

Spectroscopic absorption is translated to link-level indicators on a unified computational grid to ensure strict comparability across models and cases. The inputs consist of the two LBL-family coefficients. $\alpha_{\mathrm{LBL}}(f)$ and $\alpha_{\mathrm{LBL}\times S}(f)$ defined on $f \in [300,1000]$ GHz with $\Delta f = 0.05$ GHz. AM v14 and ITU-R P.676 absorptions are evaluated and computed for context on the identical frequency grid; they are not blended into the link computation, which is performed exclusively with $\alpha_{\mathrm{LBL}}(f)$ and $\alpha_{\mathrm{LBL}\times S}(f)$ to isolate sensitivity to continuum calibration.

Propagation is modeled as clear-air, line-of-sight transmission without multipath fading, hydrometeors, aerosols, or particulate scattering, and without hardware non-idealities (no pointing errors, phase noise, or RF non-linearities). Radio parameters are held fixed to avoid conflating propagation with equipment choices:

$$\mathrm{EIRP} = 55 \text{ dBm}, \qquad G_{\mathrm{rx}} = 50 \text{ dBi},$$
$$B = 1 \text{ GHz}, \qquad \mathrm{NF} = 6 \text{ dB},$$
$$T_{\mathrm{sys}} = 290 \text{ K}.$$

Three path lengths are considered, $L \in \{100,500,1000\}$ m, and five canonical windows structure the analysis—Z1 (300–375 GHz), Z2 (385–440 GHz), Z3 (460–525 GHz), Z4 (620–710 GHz), and Z5 (820–900 GHz).
The mapping from absorption to link metrics is explicit and unit consistent. Let $\alpha(f)$ denote a power-attenuation coefficient in m^{-1}. Over a path L (m), the gaseous loss is

$$A_{\mathrm{atm}}(f,L) = \frac{10}{\ln 10}\,\alpha(f)\,L \;\approx\; 4.342945\,\alpha(f)\,L \quad \text{(dB)},$$

and the free-space loss (with f in Hz) is

$$\mathrm{FSPL}(f,L) = 20\log_{10}(4\pi fL/c) \quad \text{(dB)}.$$

The received level follows as

$$\mathrm{RSL}(f) = \mathrm{EIRP} + G_{\mathrm{rx}} - \mathrm{FSPL}(f, L) - A_{\mathrm{atm}}(f, L) \quad (\mathrm{dBm}),$$

and the thermal-noise power over bandwidth B is

$$N_{\mathrm{dBm}} = -174 + 10\log_{10}B + \mathrm{NF} + 10\log_{10}\left(T_{\mathrm{sys}}/290\right) \quad (\mathrm{dBm}).$$

Hence,

$$\mathrm{SNR}(f) = \mathrm{RSL}(f) - N_{\mathrm{dBm}} \quad (\mathrm{dB}),$$

$$C(f) = \frac{B}{10^9}\log_2\left(1 + 10^{\mathrm{SNR}(f)/10}\right) \quad (\mathrm{Gb/s}).$$

A conservative demodulation marker (e.g., $\mathrm{SNR}_{\min} = 6$ dB) may be overlaid when needed for orientation; nevertheless, capacity is reported in its continuous form so that atmospheric effects remain visible without presupposing a specific modem.

All computations use the identical frequency grid for $\alpha_{\mathrm{LBL}}(f)$, $\alpha_{\mathrm{LBL}\times S}(f)$, AM and ITU-R, preventing interpolation bias in spectral comparisons. The guarded scaling $S(f)$ remains foreign-only, windowed (600–980 GHz), damped ($\gamma = 0.60$), and activated solely under foreign-continuum dominance (threshold 0.60), thereby avoiding artificial changes in line-dominated bands (Z1–Z3) and restricting sensitivity tests to regions where the continuum physically governs performance (Z4/Z5). This protocol yields a reproducible, case-by-case mapping from spectroscopic absorption to RSL, SNR, and $C(f)$ under a single, coherent set of assumptions.

2.3. Case Definitions and Atmospheric Conditions

2.3.1. Atmospheric State and Geometry

The propagation medium is a near-surface, horizontally homogeneous layer at $T = 296$ K and $P \approx 1013$ hPa. Dry-air composition follows the standard. N_2/O_2 abundances; temperature and pressure dependencies in line shapes are handled by the LBL solver described in §2.1.

[12] Propagation is modeled as a horizontal, Line-of-Sight (LOS) path in a single atmospheric layer (no vertical stratification within the link), an idealization that isolates spectroscopic effects from meteorological variability and is adequate for the short ranges considered. Three nominal path lengths are reused across all scenarios for comparability: $L \in \{100, 500, 1000\}$ m.

2.3.2. Humidity Cases (Water-Vapor Burden)

Water-vapor loading is varied across three controlled scenarios at the above (T, P). For each case, the H_2O Volume-Mixing Ratio (VMR) and the implied density ρ_w They are fixed and used consistently in all model families (LBL, LBL× $S(f)$, AM, ITU).

Table 1. Humidity cases

Case	Qualitative label	VMR(H_2O)	ρ_w (g·m^{-3})	State
1	Dry/low humidity	0.00485	≈ 3.60	Lower-bound burden to probe minimal continuum influence.
2	Moderate humidity	0.01080	≈ 8.01	Mid-range burden typical of mild outdoor conditions.
3	Humid/high humidity	0.02020	≈ 14.98	Upper-range burden to stress continuum sensitivity.

Densities are computed at 296 K and archived for reproducibility. These brackets do not claim to span all climates; they serve as controlled test atmospheres for sensitivity analysis. The model inputs for the H_2O continuum (MT_CKD self/foreign) is generated or read at the exact case conditions $(T, P,$ VMR) and interpolated to the standard grid.

2.3.3. Frequency Grid and Analysis Windows

All spectra are evaluated on the common grid $f \in [300,1000]$ GHz with $\Delta f = 0.05$ GHz and aggregated over five canonical windows: Z1: 300–375 GHz; Z2: 385–440 GHz; Z3: 460–525 GHz; Z4: 620–710 GHz; Z5: 820–900 GHz. Windows Z4–Z5 are the primary loci of continuum sensitivity, whereas Z1–Z3 document regimes where discrete lines dominate and the scaling is typically dormant (per the activation logic in §2.1). For compact tabulations, each window is associated with its mid-frequency $f_c = 1/2\,(f_{\mathrm{low}} + f_{\mathrm{high}}$Full-band spectra remain the authoritative view.

2.3.4. Model Families (Comparability)

For every humidity case and each frequency sample, absorptions are calculated and stored as follows: (1) LBL: $\alpha_{\mathrm{LBL}} = \alpha_{\mathrm{lines}} + \alpha_{\mathrm{self}} + \alpha_{\mathrm{foreign}} + \alpha_{\mathrm{dry}}$. (2) LBL× $S(f)$: identical decomposition, except the foreign continuum is multiplied by the Guarded Scale $S(f)$ defined in §2.1 (Windowed, Dominance-Masked, and Clamped). (3) AM and ITU-R P.676: evaluated and used as External Spectral References (AM-prioritized with ITU fallback). These last are not blended into the link mapping, which is applied to the LBL pair only.

2.3.5. Data Artifacts for Reproducibility (No Numerical Outcomes Here)

The pipeline exports, per case and distance:

- Spectral overlays $\alpha(f)$ for LBL, LBL× S, AM, and ITU with window markers over 300–1000 GHz.
- Arrays of path attenuation $A_{\mathrm{atm}}(f, L)$ derived from $\alpha(f)$ (Beer–Lambert) for subsequent FSPL/RSL/SNR/C calculations.

- Indices to f_c in each window for concise Δ-metrics; and
- CSV logs of spectral means (e.g., $\langle\alpha_{\text{self}}\rangle$, $\langle\alpha_{\text{foreign}}\rangle$, foreign fraction) documenting where the scaling mask is active.

3. Results and Discussion

This section translates the spectral modeling of Section 2 into link-level outcomes under fixed radio assumptions (EIRP $= 55$ dBm, $G_{\text{rx}} = 50$ dBi, $B = 1$ GHz, NF $= 6$ dB, $T_{\text{sys}} = 290$ K). Unless explicitly stated otherwise, all link-level comparisons refer to LBL versus LBL $\times\, S(f)$. The AM and ITU curves serve strictly as spectral references and are not projected into link metrics. The analysis is organized to highlight where the foreign-continuum Scaling $S(f)$ is active and how that activation affects Received Signal Level (RSL), SNR, and Shannon Capacity $C(f)$.

3.1. Spectral Overview and Activation of $S(f)$

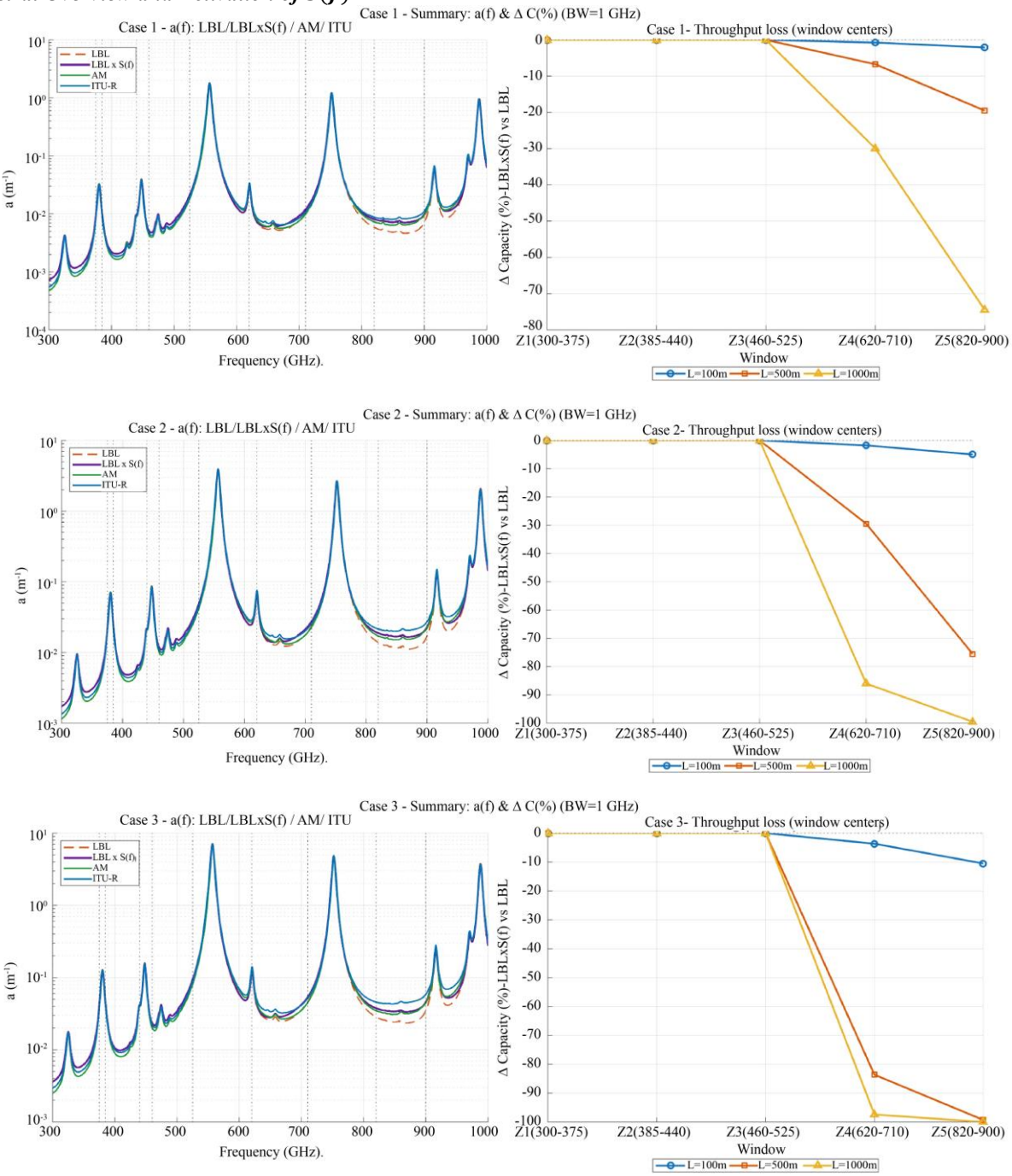

Fig. 1 THz band (0.3–1 THz) and study windows Z1–Z5

Figure 1 shows, for the three humidity cases, absorption spectra (left) and relative capacity change at each window center (right). As intended by the guard design of $S(f)$ (raised-cosine support $\approx$ 600–980 GHz and activation only where the foreign continuum dominates), the curves are indistinguishable in Z1–Z3 (300–525 GHz); these bands remain line-dominated, and the center deltas stay at $\Delta C \approx 0$ for $100/500/1000$ m across all conditions.

In Z4 (620–710 GHz), activation is partial outside strong lines, so the center, often located in a relatively line-free pocket, shows limited change at 100 m but reveals a clear distance dependence (ΔRSL, in dB):

Dry case: -1 $(100/500/1000$ m); Moderate case: ≈ 0
Humid case: -5.

This pattern reflects a slight elevation of the inter-line floor, which grows increasingly significant with path length. In Z5 (820–900 GHz), where the foreign continuum dominates, activation is widespread. The correction indicates a substantial underestimation of the continuum background in the uncorrected LBL model. (ΔRSL, in dB):

Dry: -4 Moderate: -7 Humid: -10 $(100/500/1000$ m)

Across all composites, the positions and depths of line notches are preserved (thanks to the line-neutral nature of the correction). At the same time, the continuum level is selectively lifted and entirely consistent with the intended role of $S(f)$ as a spectroscopically grounded adjustment.

The practical implication is direct: changes that appear negligible at 100 m evolve over 500 to 1000 m into multi-dB reductions of received level (since even a few 10^{-3} m^{-1} in α accumulate with distance), which in turn produce non-linear penalties in throughput. These are negligible in Z1–Z3, increasingly sensitive to humidity and range in Z4, and critical in Z5.

3.2. Link-Level Behavior: Capacity and Received Level

Building on 3.1, the link-level curves confirm that the guarded correction $S(f)$ is line-neutral: line notches and passband edges remain aligned between LBL and LBL×S; the only change is a smooth elevation of the inter-line floor wherever the foreign continuum dominates. This spectral uplift translates at the link into a distance-scaled penalty on the received level,

$\Delta\mathrm{RSL}(f, L) \simeq 4.343\,[\alpha_{\mathrm{LBLS}}(f) - \alpha_{\mathrm{LBL}}(f)]\,L$ dB, and, through SNR, into a non-linear compression of $C(f)$. The three cases below follow exactly the activation pattern established in § 3.1 (no effect in Z1–Z3; partial in Z4; broad in Z5).

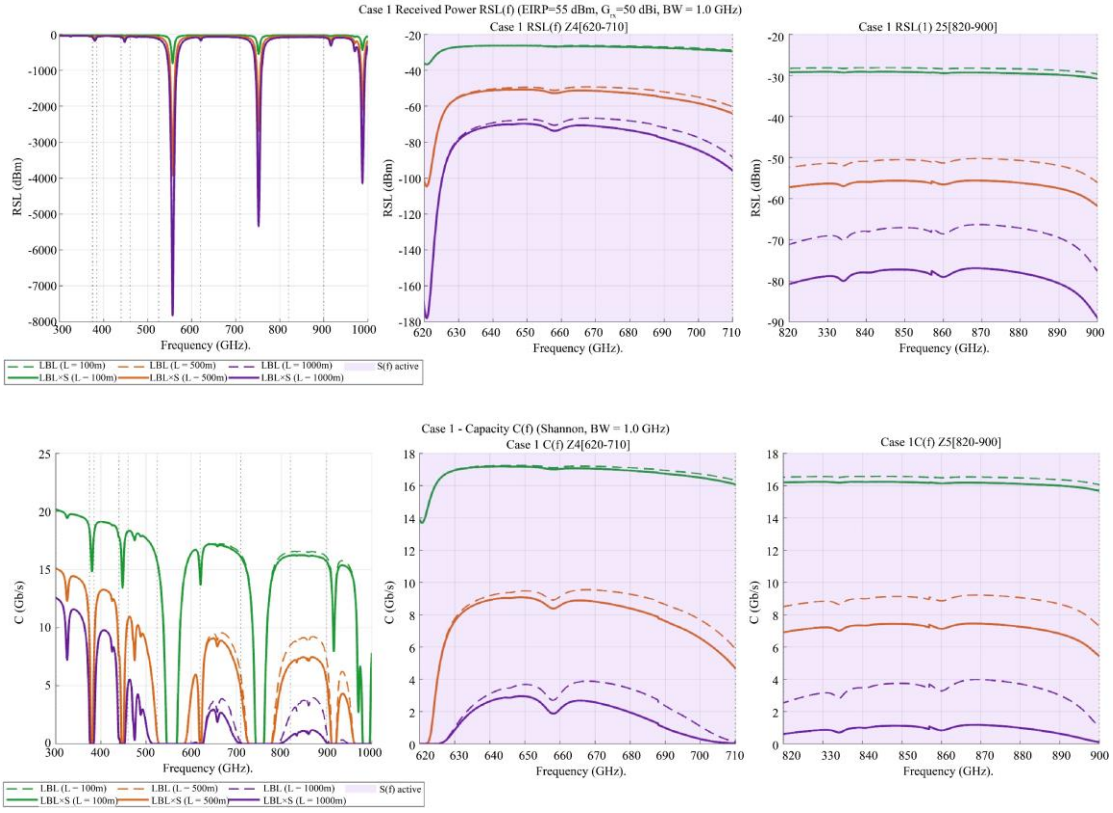

Fig. 2 Spectral Overlays & Center-Capacity Deltas — Case 1 (Dry)

For the dry case 1, in the global views, the two models are nearly indistinguishable at 100 m, with Z4 and Z5 yielding around 16–20 Gb/s. In the Z4/Z5 zoom panels, a slight vertical offset begins to appear but remains inconsequential at this range.

At 500 m, the divergence starts to have practical consequences: in Z4, the capacity curve touches the 8 Gb/s reference line for LBL and dips just below it for LBL×S; in Z5, LBL holds between 6–8 Gb/s, while LBL×S drops below the 8 Gb/s guide, indicating an approaching modulation downgrade. At 1 km, both windows are compressed to no more than 5 Gb/s. The center-frequency RSL offsets quantify the correction's impact without distorting the spectral shape: Z4 shows −0.39/−1.93/−3.87 dB, and Z5 shows −1.05/−5.23/−10.45 dB at 100/500/1000 m, respectively. In short, under dry conditions, the correction reduces the performance margin rather than usability at short ranges; the Z4 remains viable up to around 500 m, whereas the Z5 becomes increasingly throughput-sensitive beyond that distance.

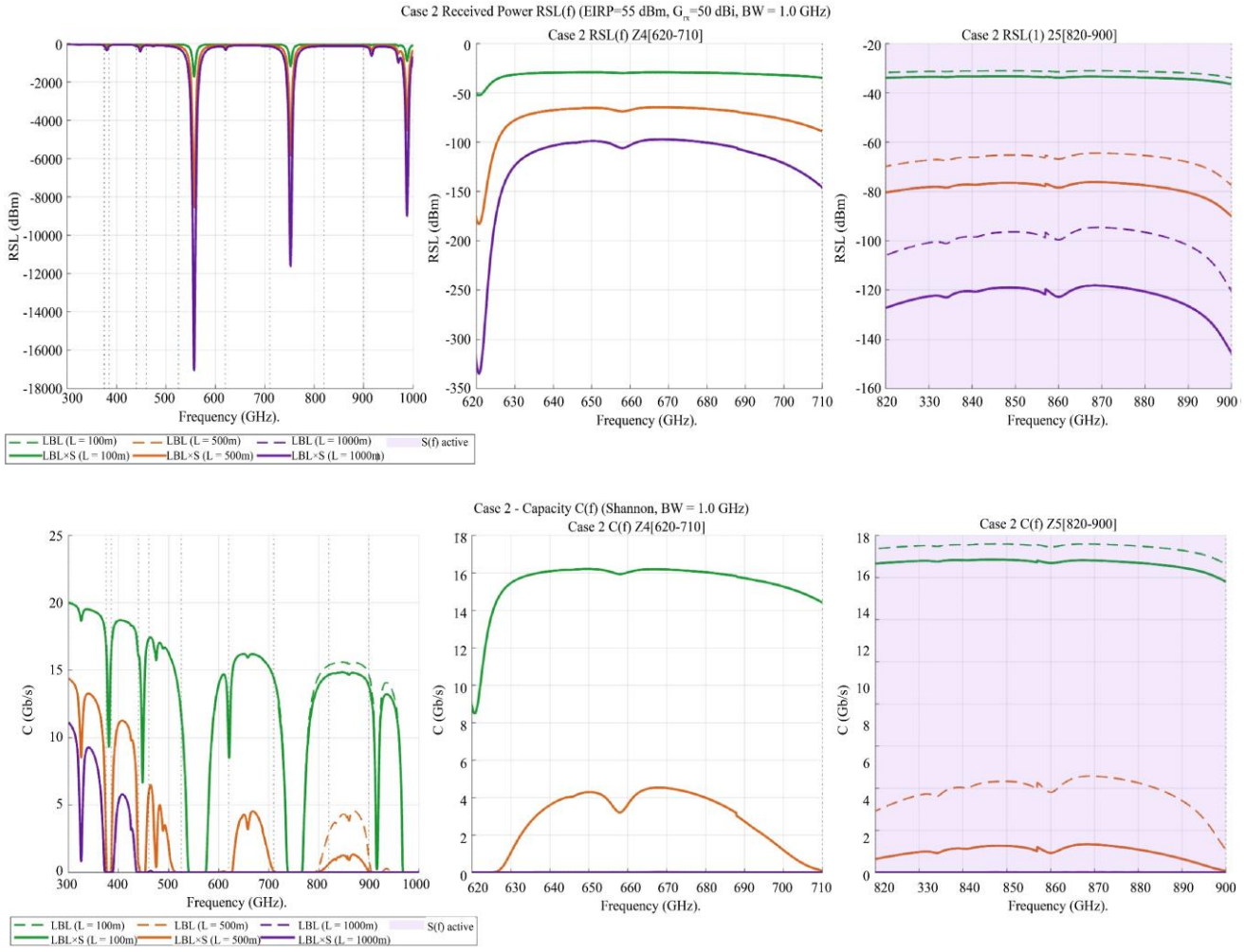

Fig. 3 Spectral Overlays & Center-Capacity Deltas — Case 2 (Moderate)

Case 2 (Moderate Humidity). — At 100 m, the Z4 and Z5 panels still display high, closely grouped capacity values, consistent with the modest center deltas noted in § 3.1.

However, by 500 m, the continuum uplift described earlier becomes clearly visible at the link level: Z4 collapses to approximately 4–6 Gb/s (with LBL×S generally not exceeding 5 Gb/s), and Z5 drops further to just 0–2 Gb/s. At 1 km, both windows are essentially shut down. The center-frequency RSL deltas in Z5 are -2.31 dB, -11.57 dB, and -23.14 dB at 100/500/1000 m, respectively, reflecting this steep decline. Meanwhile, Z4 stays relatively stable at 100 m but starts degrading with distance, as its outer flanks, where $S(f)$ activates, begin to dominate the average window behavior.

As suggested by Figure 1, even minor background discrepancies of a few $10^{-3}\ \mathrm{m}^{-1}$ accumulate with range, turning into multi-dB gaps in RSL and leading to the practical disappearance of Z4 and Z5 beyond a few hundred meters.

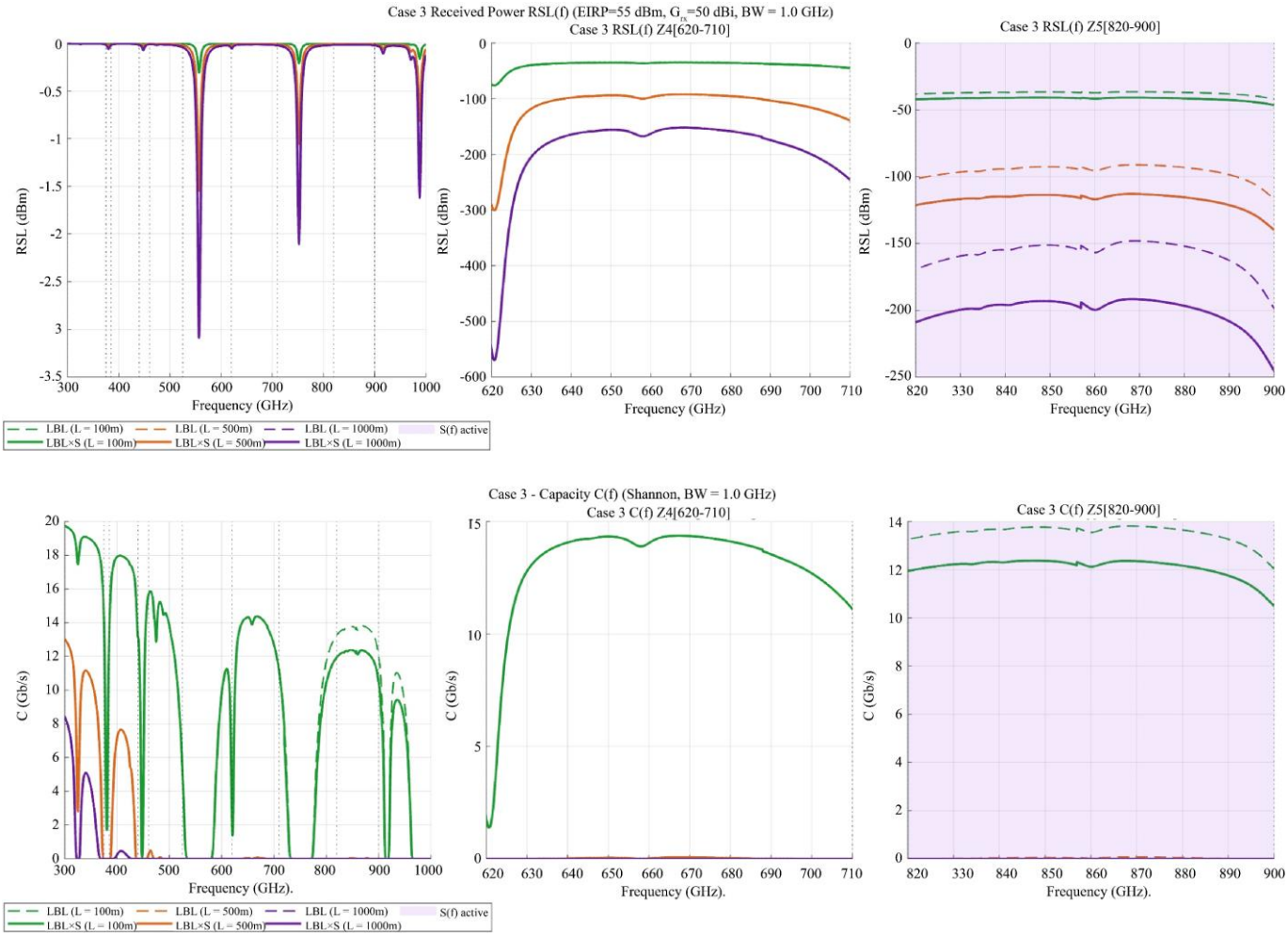

Fig. 4 Spectral Overlays & Center-Capacity Deltas — Case 3 (Humid)

Case 3 highlights the continuum-driven nature of the correction, bringing it into complete focus. At 100 m, Z4 still supports approximately 10–15 Gb/s and Z5 around 10–12 Gb/s, with LBL×S following a similar shape but tracing a slightly lower envelope. From 500 m onward, both windows collapse to near-zero capacity and remain that way at 1 km. The center-frequency losses in Z5 are −4.29/−21.43/−42.87 dB and align fully with the broad activation pattern described in § 3.1, and with the correction's line-neutral property: the spectral notches remain identical, but LBL×S sits consistently on a lower absorption floor. In effect, under humid conditions, the usability of Z4 and Z5 becomes limited to short ranges under the nominal radio assumptions, while the lower windows (Z1–Z3) retain the robustness observed in previous cases.

Across all three scenarios, the figures thus offer a coherent transition from the where and how much identified spectrally in § 3.1 to the how far and how fast at the link level: Z1–Z3 remain unaffected; Z4 shows compression that scales with distance and humidity (mild in dry air, severe otherwise); and Z5, being strongly continuum-dominated, undergoes the most significant reduction in margin; negligible at 100 m, but decisive between 500 and 1000 m.

3.3. SNR Evolution and Achievable Transmission Rates

The distance–frequency plots of SNR are built on the analysis from §3.1–3.2 by converting the spectral corrections into concrete indicators of link feasibility. The dashed horizontal lines set at 6 dB for QPSK 3/4 and 24 dB for 64-QAM ¾ act purely as visual references: they mark typical demodulation thresholds for a 1 GHz bandwidth and allow for a quick assessment of which frequency regions remain viable as distance and humidity increase.

In the dry atmosphere (Case 1), SNR values in Z1–Z3 consistently stay above 30 dB across all distances, reinforcing the notion that line-dominated bands are largely unaffected by continuum scaling. In the Z4 (620–710 GHz) range, the curves start at around 35 dB at 100 m and remain close to or above the 24 dB threshold up to 500 m, indicating that higher-order modulations are still achievable under both modeling approaches.

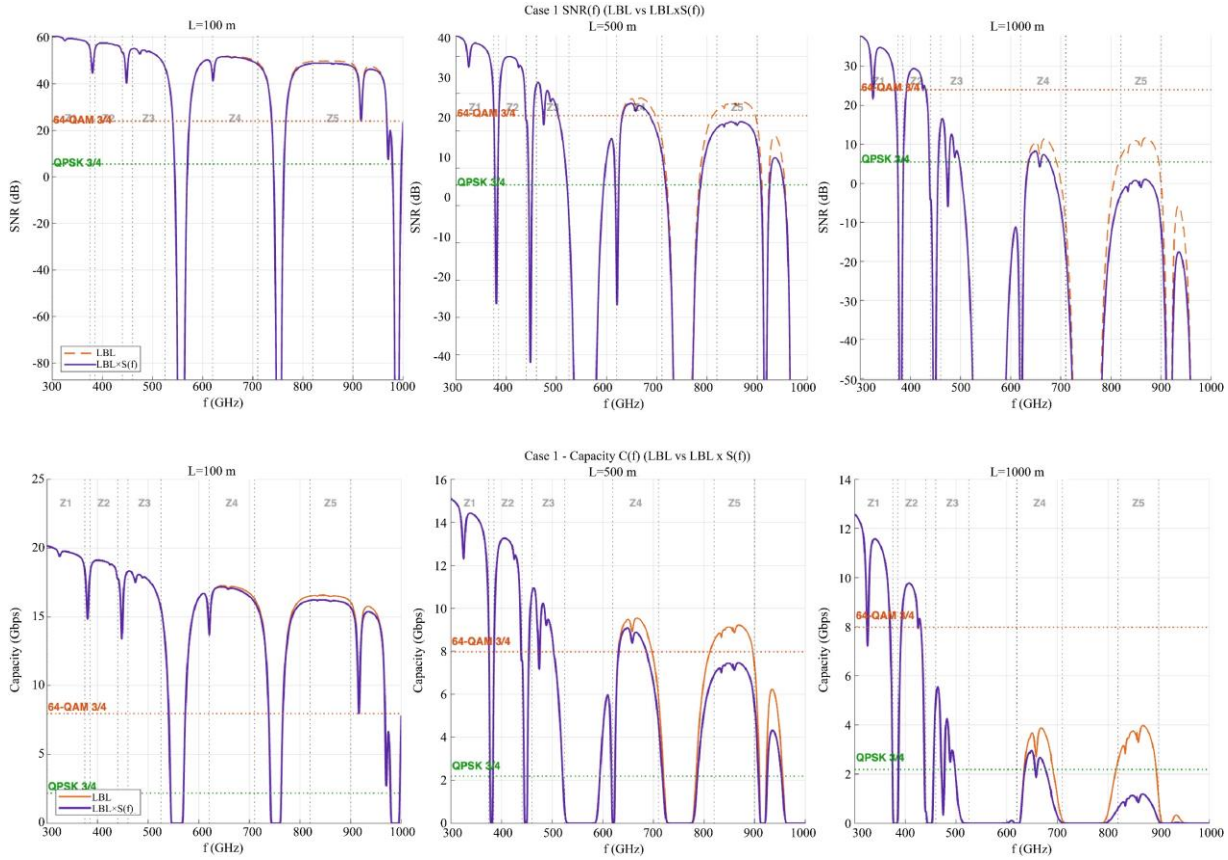

Fig. 5 SNR, Distance, Shannon Capacity vs Frequency — Case 1 (Dry)

At 1 km, SNR values drop to between 5 and 7 dB, effectively limiting the link to robust, low-rate modulation schemes. The difference between LBL and LBL×S stays within 2 dB, aligning with the modest background correction observed in the spectral domain.

Z5 (820–900 GHz), by contrast, proves more sensitive. At 100 m, both models exceed 24 dB, but by 500 m, the LBL×S curve has declined to around 18–20 dB, while LBL remains closer to 25 dB, shifting the system from 64-QAM toward QPSK operation. At 1 km, this band drops to near or below 6 dB SNR under LBL×S, indicating that the corrected model is nearing outage conditions.

In the moderate humidity scenario (Case 2), Z1–Z3 once again show no observable degradation. However, the difference between LBL and LBL×S becomes more pronounced in the upper windows. Z4 still holds around 30 dB at 100 m, but SNR falls off quickly with distance: by 500 m, LBL×S averages between 6 and 8 dB, while LBL hovers near 10 dB, meaning only low-rate transmission remains feasible. Z5 deteriorates even faster by 500 m, SNR under LBL×S barely reaches 5 dB, and the capacity curves flatten below 2 Gb/s, leaving little room for any practical high-order modulation. At 1 km, both Z4 and Z5 fall entirely below 0 dB, matching the $\Delta C \approx -100$ % reported earlier.

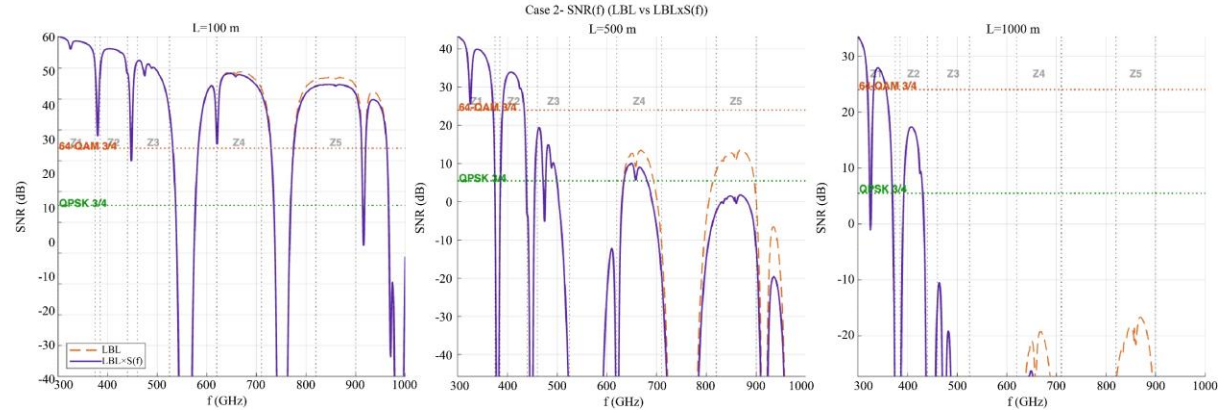

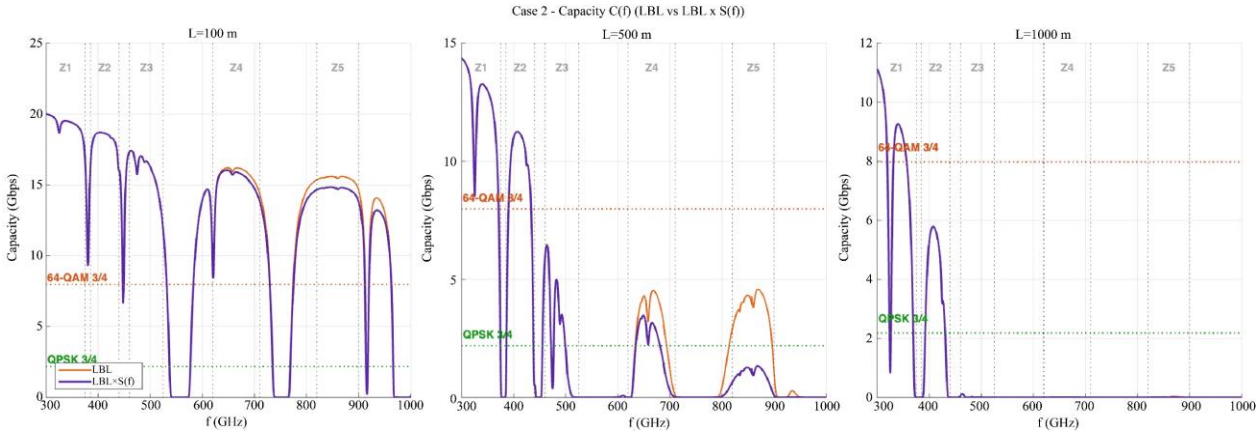

Fig. 6 SNR, Distance, Shannon Capacity vs Frequency — Case 2

Under humid air conditions (Case 3), the correction has a clearly decisive effect. Although Z4 and Z5 still deliver SNR values above 24 dB and capacities in the range of 12 to 16 Gb/s at 100 m, both bands collapse beyond 500 m, with SNR dropping below 0 dB across most of the 600–900 GHz spectrum. The LBL and LBL×S curves remain parallel, once again confirming the line-neutral nature of the correction, but are vertically offset by more than 10 dB at 500 m and over 20 dB at 1 km.

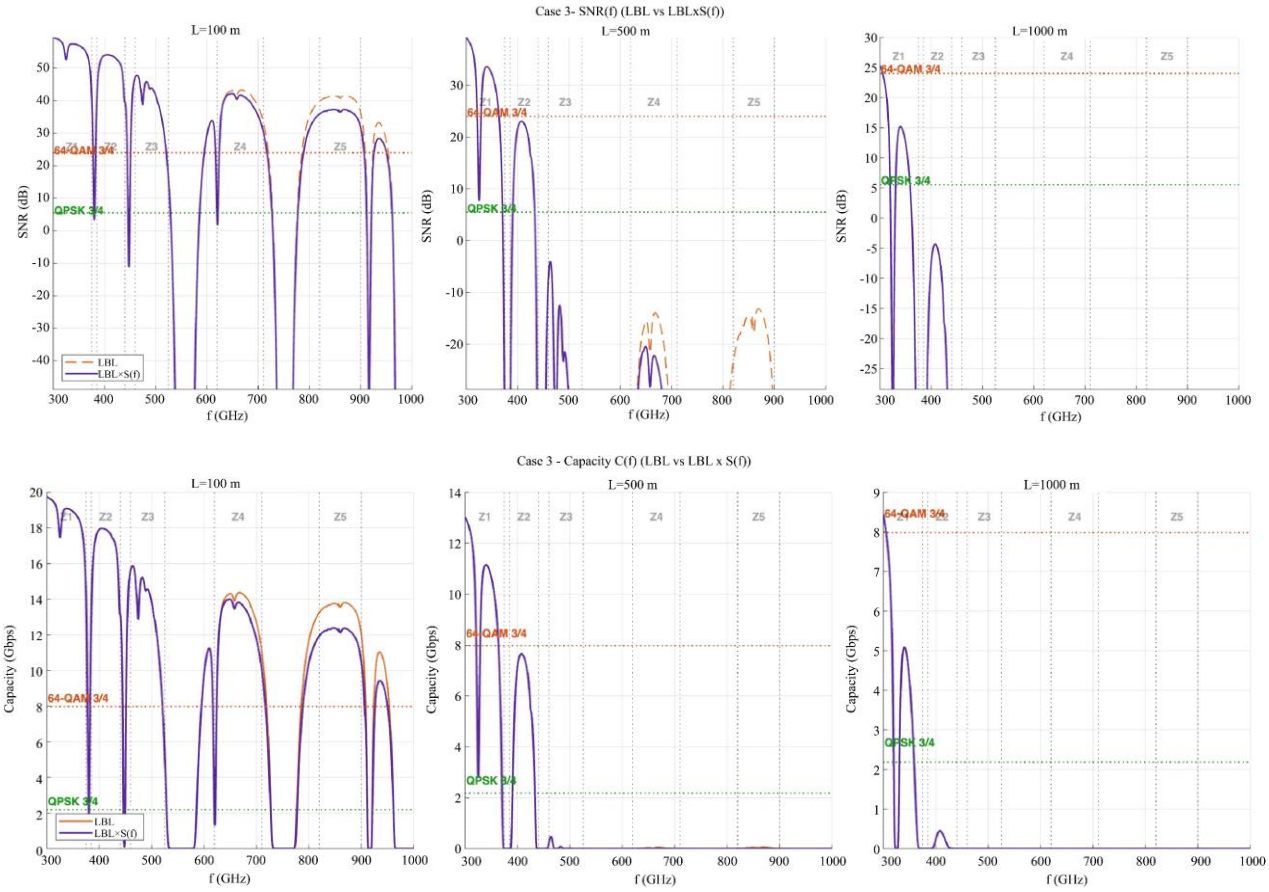

Fig. 7 SNR, Distance, Shannon Capacity vs Frequency — Case 3 (Humid)

The conclusion is unambiguous: under humid conditions, only the lower frequency windows remain usable beyond a few hundred meters, while the upper bands are reduced to short-range options, viable only over tens to low hundreds of meters.

Viewed together, Figures 5 through 7 show that the spectral

correction introduced in Ref. [3] consistently carries through the entire link chain. Minor absorption differences are barely noticeable in the α-plots at 100 m and lead to gradual, case-dependent reductions in SNR that ultimately define the usable range of each THz window: below 600 GHz, links remain stable and broadband; around 700 GHz, performance becomes distance-limited; and above 800 GHz, links are confined to short-range scenarios. The available margin decreases with humidity, following the activation pattern of S(f) exactly as anticipated.

3.4. Link-level Synthesis and Engineering Implications

The cross-case synthesis confirms the internal consistency of all previous results: the line-by-line correction S(f) leaves the spectral structure intact, yet significantly redefines the usable margins of a THz link once distance and humidity are factored in. The quantitative summary (covering ΔC%, RSL, and SNR at the Z4–Z5 centers) shows a penalty that increases almost proportionally with both path length and water-vapor density. In dry conditions, the additional absorption remains minimal below 500 meters, keeping Z4 operational and only moderately impacting Z5. Under moderate humidity, both windows show capacity losses exceeding 10% by 500 meters and are effectively out of service at 1 km. In humid air, Z5 collapses beyond 200–300 meters, with Z4 following soon after, leaving only the lower windows (Z1–Z3) as consistently viable across the range.

From a system design perspective, these findings suggest a few straightforward guidelines:

- The lower bands (≤ 525 GHz) can be treated as reliable baselines, largely unaffected by continuum modeling uncertainties.
- The 620–710 GHz range (Z4) supports intermediate-range links spanning a few hundred meters in dry to moderate conditions but quickly becomes power-constrained when humidity increases.
- The 820–900 GHz range (Z5) is best suited to very short-range or high-gain deployments, where its wide bandwidth can offset its high atmospheric vulnerability.

In essence, S(f) does not alter line physics; it corrects a systematic underestimation of the foreign continuum that, when propagated through link-level metrics, results in multi-decibel RSL drops and order-of-magnitude capacity losses in the higher-frequency windows. [13] This establishes a direct and quantitative link between the microscopic spectroscopic precision of the model developed in Article 1 and the macroscopic design constraints of THz wireless systems.

4. Conclusion

This study has extended the line-by-line framework introduced in previous research [3], moving beyond pure spectroscopy to assess its implications at the link level. By quantifying how the empirical continuum correction $S(f)$ reshapes the feasibility of outdoor THz communications, it shows that even minor absorption biases on the order of a few 10^{-3} m^{-1}, can accumulate into multi-decibel signal losses and significant capacity drops over realistic distances. The correction operates selectively: it leaves low-frequency bands untouched but gradually constrains the 600–900 GHz region as humidity and path length increase.

A nearly linear connection with water-vapor content is revealed by the quantitative results. While still functional at 100 meters in dry air, Windows Z_4 (620–710 GHz) and Z_5 (820–900 GHz) undergo severe throughput deterioration beyond 500 meters in moderate humidity and become practically ineffective in humid situations. Bands below 600 GHz, on the other hand, continue to operate under all atmospheric conditions, demonstrating their feasibility for terrestrial broadband deployment. These patterns show a distinct operational hierarchy among THz windows, where continuum calibration accuracy rather than line-absorption uncertainty is the primary limiting factor. [14]

This has impacts for system design. Ignoring the foreign-continuum contribution or relying on models that may underestimate it can lead to link budgets that are off by several decibels. This, in turn, affects power planning, modulation strategy, and ultimately, link availability in humid environments. Continuum modeling, far from being a secondary refinement, should therefore be treated as a key environmental parameter quantified, validated, and monitored. By tying together physically consistent absorption modeling with practical metrics like RSL, SNR, and capacity, this work helps bridge a longstanding disconnect between spectroscopic accuracy and wireless system design. It provides a replicable framework for making well-informed decisions on frequency, coverage range, and climate sensitivity, ranging from high-resolution spectral data to practical link-budget budgeting. Beyond the approach, the findings highlight the necessity of fresh experimental validation of the high-frequency continuum, particularly in the 600–900 GHz region, to prevent potentially underestimating atmospheric penalties that might delay the deployment of next-generation THz networks.

References

[1] Ian F. Akyildiz, Josep Miquel Jornet, and Chong Han, "Terahertz Band: Next Frontier for Wireless Communications," *Physical Communication*, vol. 12, pp. 16–32, 2014. [CrossRef] [Google Scholar] [Publisher Link]

[2] Theodore S. Rappaport et al., "Wireless Communications and Applications Above 100 GHz: Opportunities and Challenges for 6G and Beyond," *IEEE Access*, vol. 7, pp. 78729–78757, 2019. [CrossRef] [Google Scholar] [Publisher Link]

[3] Ahmed Sidi Aman, and Ramafiarisona Hajasoa Malala, "Physically Transparent LBL Modeling of 0.3–1 THz Attenuation: Windowed Foreign-Continuum Scaling and Validation," *International Journal of Computer Trends and Technology (IJCTT)*, vol. 73, no. 8, pp. 33–40, 2025. [CrossRef] [Publisher Link]

[4] Domenico Cimini et al., "Uncertainty of Atmospheric Microwave Absorption Model: Impact on Ground-based Radiometer Simulations and Retrievals," *Atmospheric Chemistry and Physics*, vol. 18, no. 20, pp. 15231–15259, 2018. [CrossRef] [Google Scholar] [Publisher Link]

[5] IEEE 802.15.3d-2017, IEEE Standard for High Data Rate Wireless Multi-Media Networks Amendment 2: 100 Gb/s Wireless Switched Point-to-Point Physical Layer, 2017. [Google Scholar] [Publisher Link]

[6] I.E. Gordon et al., "The HITRAN2020 Molecular Spectroscopic Database," *Journal of Quantitative Spectroscopy and Radiative Transfer*, vol. 277, 2022. [CrossRef] [Google Scholar] [Publisher Link]

[7] Eli J. Mlawer et al., "Development and Recent Evaluation of the MT_CKD Model of Continuum Absorption," *Philosophical Transactions of the Royal Society A*, vol. 370, no. 1968, 2012. [CrossRef] [Google Scholar] [Publisher Link]

[8] P Series Radiowave Propagation, Attenuation by Atmospheric Gases and Related Effects, Recommendation ITU-R P.676-12, International Telecommunication Union, 2019. [Google Scholar] [Publisher Link]

[9] Scott Paine, "The Am Atmospheric Model," *Zenodo,* 2024. [CrossRef] [Google Scholar] [Publisher Link]

[10] ITU-R Recommendation P.525-4, Calculation of Free-space Attenuation, 2019. [Publisher Link]

[11] Andrea Goldsmith, *Wireless Communications*, Cambridge University Press, 2005. [Google Scholar] [Publisher Link]

[12] ITU-R Recommendation P.835-7, Reference Atmospheres, 2024. [Publisher Link]

[13] M. Yu. Tretyakov et al., "Atmospheric Water-vapor Continuum Model for the Sub-THz Range," *Journal of Quantitative Spectroscopy and Radiative Transfer*, vol. 333–334, 2025. [CrossRef] [Google Scholar] [Publisher Link]

[14] Emma Turner et al., "Literature Review on Microwave and Sub-millimetre Spectoscopy for Metop Second Generation," *Numerical Weather Prediction*, 2022. [Publisher Link]